J|A|C|S
ARTICLES
Published on Web 03/11/2003

Protein Side-Chain Motion and Hydration in Proton-Transfer Pathways. Results for Cytochrome P450cam

Srabani Taraphder† and Gerhard Hummer*

Contribution from the Laboratory of Chemical Physics, National Institute of Diabetes and Digestive and Kidney Diseases, National Institutes of Health, Bethesda, Maryland 20892-0520

Received August 16, 2001; E-mail: gerhard.hummer@nih.gov

Abstract: Proton-transfer reactions form an integral part of bioenergetics and enzymatic catalysis. The identification of proton-conducting pathways inside a protein is a key to understanding the mechanisms of biomolecular proton transfer. Proton pathways are modeled here as hydrogen bonded networks of proton-conducting groups, including proton-exchanging groups of amino acid side chains and bound water molecules. We focus on the identification of potential proton-conducting pathways inside a protein of known structure. However, consideration of the static structure alone is often not sufficient to detect suitable proton-transfer paths, leading, for example, from the protein surface to the active site buried inside the protein. We include dynamic fluctuations of amino acid side chains and water molecules into our analysis. To illustrate the method, proton transfer into the active site of cytochrome P450cam is studied. The cooperative rotation of amino acids and motion of water molecules are found to connect the protein surface to the molecular oxygen. Our observations emphasize the intrinsic dynamical nature of proton pathways where critical connections in the network may be transiently provided by mobile groups.

Introduction

Protein-mediated proton transfer is of fundamental importance in bioenergetics[1−3] and enzyme catalysis.[4,5] Understanding the energetics and kinetics of proton delivery into and through the active site of proteins is thus an essential element of quantitative descriptions of biomolecular function. A prerequisite for such descriptions is the identification and characterization of proton-conducting pathways inside proteins. Finding such pathways is the focus of the present article.

Proton conduction in liquid water is widely believed to occur through hydrogen bonded networks of water molecules, as envisaged by de Grotthuss based on his pioneering study of water electrolysis,[6] but detailed molecular mechanisms are still actively investigated.[7−9] For long-range proton transfer in proteins, additional complications arise from the structural inhomogeneity and dynamical complexity of the medium, with several factors affecting the transfer kinetics, including fluctuations in proton affinities, donor and acceptor distances, and the dielectric response. A common starting point in biomolecular proton transfer is again the assumption of a Grotthuss-like charge relay mechanism where the proton is translocated via hydrogen bonded networks[10,11] of polar amino acid side chains and bound water molecules.[12] The molecular mechanism for proton conduction along hydrogen bonded chains ("proton wires") or networks involves two key steps: translocation of an excess proton (propagation of an ionic defect) and reorientation of the hydrogen bonded chain or network (termed usually as the "bonding defect"). The difference in proton affinities is measured in terms of pK_a values of the participating groups[5,13−15] and exerts energetic control over each proton-transfer step. For a given donor−acceptor pair, this driving force may be significantly different from that observed in bulk solution, as even small environmental perturbations are known to cause marked pK_a shifts.[16]

Representation of proton-transfer networks using kinetic equations[17−19] provides a phenomenological characterization of their transport properties. In essence, the kinetic models assume (1) specific protonation states of the proton-conducting groups with (2) free energy values assigned according to the pK_a values to define the equilibria between states. The derivation of the proton-transfer kinetics is usually based on transition state theory

† Permanent address: Department of Chemistry, Indian Institute of Technology, Kharagpur 721302, India.

(1) Mitchell, P. *Nature* **1961**, *191*, 144.
(2) Gennis, R. B. *Biomembranes*: *Molecular Structure and Function*; Springer-Verlag: New York, 1989.
(3) Wikström, M. *Curr. Opin. Struct. Biol.* **1998**, *8*, 480.
(4) Silverman, R. B. *The Organic Chemistry of Enzyme Catalyzed Reactions*; Academic Press: New York, 2000.
(5) Warshel, A. *Computer Modelling of Chemical Reactions in Enzymes and Solutions*; John-Wiley: New York, 1997.
(6) de Grotthuss, C. J. T. *Annal. Chim.* **1806**, *58*, 54.
(7) Agmon, N. *Chem. Phys. Lett.* **1995**, *244*, 456.
(8) Geissler, P.; Dellago, C.; Chandler, D.; Hutter, J.; Parrinello, M. *Science* **2001**, *291*, 2121.
(9) Day, T. J. F.; Schmitt, U. W.; Voth, G. A. *J. Am. Chem. Soc.* **2000**, *122*, 12027.
(10) Onsager, L. In *The Neurosciences*; Quarton, G., Melnechuk, T., Schmitt, F. O., Eds.; Rockefeller University Press: New York, 1967; pp 75−79.
(11) Nagle, J. F.; Morowitz, H. J. *Proc. Natl. Acad. Sci. U.S.A.* **1978**, *75*, 298.
(12) Pomès, R.; Roux, B. *Biophys. J.* **1996**, *71*, 19.
(13) Antosiewicz, J.; Briggs, J. M.; Elcock, A. H.; Gilson, M. K.; McCammon, J. A. *J. Comput. Chem.* **1996**, *17*, 1633.
(14) Sham, Y. Y.; Chu, Z. T.; Warshel, A. *J. Phys. Chem. B* **1997**, *101*, 4458.
(15) Alexov, E. G.; Gunner, M. R. *Biochemistry* **1999**, *38*, 8253.
(16) Sampogna, R. V.; Honig, B. *Biophys. J.* **1994**, *66*, 1341.
(17) Knapp, E. W.; Schulten, K.; Schulten, Z. *Chem. Phys.* **1980**, *46*, 215.
(18) Brünger, A.; Schulten, Z.; Schulten, K. *Z. Physikal. Chem.* **1983**, *136*, 1.
(19) Schulten, Z.; Schulten, K. *Methods Enzymol.* **1986**, *127*, 419.

10.1021/ja016860c

with (3) molecular mechanisms, such as rotation of hydrogen bonding groups or proton transfer between donor and acceptor, connecting the states with (4) specific energy barriers for each of the mechanisms converting between different states. The kinetics of proton transfer between a donor and an acceptor may be estimated within the framework of Marcus theory.[20,21] But, implementation of such a model in biomolecular systems faces problems regarding, for example, the identification of specific protonation states of the proton-conducting groups and the estimation of the free energy of activation along the reaction coordinate. The kinetic model is particularly useful if the proton is sequentially relayed through a network so that the reaction coordinates and free energy barriers for each step are well-defined. But, it is not easily applicable if proton translocation is associated with the concerted motion of several groups where no simple reaction coordinate can easily be identified. Experimental studies of proton conduction through hydrogen bonded chains indeed reveal broad features in the infrared spectra attributed to collective proton tunneling.[22] Additional complications arise as the transfer kinetics along a path may not necessarily be limited by the rate of intrinsic proton transfer between a given donor and acceptor pair. Instead, slow steps may involve the formation of efficient proton-conducting pathways. The latter is expected to derive significant contributions from the dynamics of protein structure and internal water molecules, thus making the kinetic analysis a formidable challenge.

Here, the goal is to identify hydrogen bonding networks inside a protein as potential proton-conducting pathways. In biological electron-transfer reactions,[23,24] numerous pathways may coexist principally because of the high tunneling rates of electrons. In contrast, because of the relatively large proton mass and the correspondingly reduced quantum mechanical tunneling rates, the number of pathways efficient in transferring protons is intrinsically small. Analysis of high resolution crystal structures of proteins typically yields fragmented proton-transfer pathways[25,26] that do not extend from the surface to the active site of the protein. The actual pathways may be dynamic in origin and result from cooperative fluctuations in protein structure and interior hydration.[27−30] Dynamic fluctuations in the protein structure may arise, for example, from local side-chain motion, secondary structure movement, loop closing, and hinge bending.[31] These fluctuations can affect proton affinities[15] and establish connections between proton-conducting groups otherwise unconnected. These dynamic processes span time scales of several orders of magnitude.[31] Coupling of these fluctuations to the hydration of the protein may lead to further complications. Interior water molecules are expected to play a significant role in establishing proton-conducting pathways, including (i) isolated water molecules that bridge between amino acid residues but do not interact with other water molecules, (ii) linear chains of water molecules,[11,12,17,22,32] (iii) branching networks of water molecules and proton-conducting amino acids,[33,34] (iv) channels filled with many water molecules forming extensively connected and possibly fluidlike fluctuating networks,[28,30,35] and (v) water molecules that transiently occupy hydrophobic cavities.[36−41] Dynamic fluctuations in the protein structure can lead to inward diffusion of water molecules from the surface,[42] thus transiently providing additional hydrogen bonding partners to the network. Such transient hydration of hydrophobic regions appears to be relevant in the proton access channels of both bacteriorhodopsin and cytochrome *c* oxidase.[3,40,41] At present, it seems prohibitively difficult to resolve the relative contributions of the different factors to the overall kinetics of proton transfer. Here, we focus on a small yet fundamental aspect by extending the network model of proton transfer through sampling of side-chain conformations and protein hydration. We then use the extended model to study proton transfer in cytochrome P450cam.

Cytochrome P450 proteins are heme-containing mono-oxygenases that catalyze the stereospecific hydroxylation of non-activated hydrocarbons at physiological temperatures.[4,43−46] These reactions, if uncatalyzed, would encounter a high activation barrier even if a nonstereospecific product is desired. The structures of several cytochrome P450 molecules have been determined crystallographically, with the camphor mono-oxygenase P450cam being the "work horse" of P450 studies.[43] Recently, high-resolution structures were obtained for several intermediates in the hydroxylation of camphor by P450cam with trapping techniques and cryo-crystallography to elucidate the details of enzyme function.[47,48] The current understanding of the reaction mechanism[43] involves a proton-assisted cleavage of the O−O bond through protonation of the distal oxygen of the heme-bound dioxygen molecule. It has been shown that the activation of the molecular oxygen depends critically on the delivery of protons to the distal oxygen atom.[49] Protonation of the proximal oxygen, in contrast, leads to "uncoupling", that

(20) Marcus, R. A. *J. Phys. Chem.* **1968**, *72*, 891.
(21) Kresge, A. J. *Acc. Chem. Res.* **1975**, *8*, 354.
(22) Brzezinski, B.; Radziejewski, P.; Zundel, G. *J. Chem. Soc., Faraday Trans.* **1995**, *91*, 3141.
(23) Beratan, D. N.; Betts, J. N.; Onuchic, J. N. *Science* **1991**, *252*, 1285.
(24) Moser, C. C.; Keske, J. M.; Warncke, K.; Farid, R. S.; Dutton, P. L. *Nature* **1992**, *355*, 796.
(25) Tsukihara, T.; Aoyama, H.; Yamashita, E.; Tomizaki, T.; Yamaguchi, H.; Shinzawa-Itoh, K.; Nakashima, R.; Yaono, R.; Yoshikawa, S. *Science* **1995**, *269*, 1069.
(26) Iwata, S.; Ostermeier, C.; Ludwig, B.; Michel, H. *Nature* **1995**, *376*, 660.
(27) Rammelsberg, R.; Huhn, G.; Lübben, M.; Gerwert, K. *Biochemistry* **1998**, *37*, 5001.
(28) Riistama, S.; Hummer, G.; Puustinen, A.; Dyer, R. B.; Woodruff, W. H.; Wikström, M. *FEBS Lett.* **1997**, *414*, 275.
(29) Deisenhofer, J.; Epp, O.; Sinning, I.; Michel, H. *J. Mol. Biol.* **1995**, *246*, 429.
(30) Hofacker, I.; Schulten, K. *Proteins: Struct., Funct., Genet.* **1998**, *30*, 100.
(31) Brooks, C.; Karplus, M.; Pettitt, B. M. *Proteins*: *A Theoretical Perspective of Dynamics, Structure, and Thermodynamics*; Wiley: New York, 1990.
(32) Pomès, R.; Roux, B. *Biophys. J.* **1998**, *75*, 33.
(33) Oprea, T. I.; Hummer, G.; García, A. E. *Proc. Natl. Acad. Sci. U.S.A.* **1997**, *94*, 2133.
(34) Ermler, U.; Fritzsch, G.; Buchanan, S. K.; Michel, H. *Structure* **1994**, *2*, 925.
(35) Pomès, R.; Hummer, G.; Wikström, M. *Biochem. Biophys. Acta Bioenerget.* **1998**, *1365*, 255.
(36) Ernst, J. A.; Clubb, R. T.; Zhou, H. X.; Gronenborn, A. M.; Clore, G. M. *Science* **1995**, *267*, 1813.
(37) Yu, B.; Blaber, M.; Gronenborn, A. M.; Clore, G. M.; Caspar, D. L. D. *Proc. Natl. Acad. Sci. U.S.A.* **1999**, *96*, 103.
(38) Helms, V.; Wade, R. C. *Proteins: Struct., Funct., Genet.* **1998**, *32*, 381.
(39) Backgren, C.; Hummer, G.; Wikström, M.; Puustinen, A. *Biochemistry* **2000**, *39*, 7863.
(40) Hummer, G.; Rasaiah, J. C.; Noworyta, J. P. *Nature* **2001**, *414*, 188.
(41) Hummer, G.; Rasaiah, J. C.; Noworyta, J. P. In *Technical Proceedings of the Second International Conference on Computational Nanoscience and Nanotechnology*; Laudon, M., Romanowicz, B., Eds.; Computational Publications: Cambridge, MA, 2002, pp 124−127.
(42) García, A. E.; Hummer, G. *Proteins: Struct., Funct., Genet.* **2000**, *38*, 261.
(43) de Montellano, O. *Cytochrome P450*: *Structure, Mechanism and Biochemistry*; Plenum-Press: New York, 1995.
(44) Hasemann, C. A.; Kurumbail, R. G.; Boddupalli, S. S.; Peterson, J. A.; Deisenhofer, J. *Structure* **1995**, *3*, 41.
(45) Sligar, S. G.; Filipovic, D.; Stayton, P. *Methods Enzymol.* **1992**, *206*, 31.
(46) Kellner, D. G.; Maves, S. A.; Sligar, S. G. *Curr. Opin. Biotechnol.* **1997**, *8*, 274.
(47) Schlichting, I.; Berendzen, J.; Chu, K.; Stock, A. M.; Maves, S. A.; Benson, D. E.; Sweet, B. M.; Ringe, D.; Petsko, G. A.; Sligar, S. G. *Science* **2000**, *287*, 1615.
(48) Denisov, I. G.; Makris, T. M.; Sligar, S. G. *J. Biol. Chem.* **2001**, *276*, 11648.
(49) Aikens, J.; Sligar, S. G. *J. Am. Chem. Soc.* **1994**, *116*, 1143.

is, production of peroxide instead of the hydroxylated product. Internal water molecules have been implicated in several aspects of the catalytic function of cytochrome P450.[47] Based on structural evidence and kinetic-solvent-isotope effects,[44,49−52] water molecules are thought to form a critical part of the proton delivery mechanism. Water molecules at the active site have also been suggested to influence the high spin to low spin equilibrium of the heme iron.[51] A cluster of water molecules hydrating the heme propionates was suggested to serve as a possible exit channel for water molecules released from the active site upon substrate binding.[33]

Recent mutation, crystallographic, and kinetic-isotope-effect studies provided evidence for a functional role of the amino acid residue Asp-251 in the proton delivery mechanism of cytochrome P450cam.[49,52,53] Mutation of Asp-251 by Asn leads to a marked decrease in the catalytic turnover of the enzyme.[52,54−56] Alternative proton pathways from the solvent into the active site of P450 may pass through the hydration cluster of the heme propionates[33] or the bound water molecules 687, 566, and 523 forming the "internal solvent channel" (numbering as in PDB structure 1dz8[47]). The latter terminates at Glu-366 without any connection to the surface.[52] Even in a high-resolution, dioxygen-bound structure of P450cam,[47] none of these pathways actually connect the distal oxygen to the surface. Moreover, none of these pathways directly require the participation of Asp-251. Therefore, the role of Asp-251 needs to be investigated in detail. Several mutagenesis studies have also explored the role of the active-site residue Thr-252 in promoting protonation of the distal oxygen. In the mutant Thr252Ala, the major products are peroxide or superoxide resulting from uncoupling.[57,58] Similar uncoupling was observed with the mutants Thr252Ile and Thr252Ala−Asp251Asn.[59] Whereas molecular dynamics suggested a role of Thr-252 as a proton donor to the distal oxygen,[60] mono-oxygenase activity was not lost when its hydroxy group was replaced by a methoxy group.[61] This suggests a participation of the oxygen atom of Thr-252 in stabilizing the dioxygen complex, but not as a direct donor to O_2. One possible explanation is that a water molecule occupying the space available in a Thr252Ala mutation might lead to an accelerated proton delivery resulting in increased hydrogen peroxide production.[62]

We will first present the theoretical method to study the effects of conformational fluctuations and the coupled variation in hydration structure of the protein interior. We will then apply this method to investigate proton delivery into the active site of cytochrome P450cam. Within the pathways involving Asp-251, we identify four alternative models. All models appear kinetically relevant on the time scale of turnover. The model with the smallest steric hindrance to side-chain motion is further supported by earlier measurements of solvent kinetic isotope effects.[52]

Theory

Hydrogen Bonded Networks. Based on the assumption that protons are translocated through proteins via hydrogen bonded networks of amino acid residues and bound water molecules, we first develop a method to identify the possible proton-translocation pathways. The thermodynamic driving force for proton transfer is quantified by a difference in pK_a values of the initial donor and final acceptor. Two elementary processes can be distinguished in long-range proton transfer: (1) transient deprotonation and protonation of two neighboring groups resulting in a temporary change of their charge states and (2) simultaneous protonation and deprotonation of a group in a Grotthuss-type proton relay without a change in its charge state. A transient change in the charge state is energetically feasible under ambient conditions if the pK_a value of the group is close to neutral as, for example, in His, Asp, or Glu amino acids in suitable environments. A Grotthuss-type concerted transfer requires that the hydrogen exchange rates of the groups involved are sufficiently high. Such proton relays can be efficient even if the pK_a values are far from neutral as, for example, in Ser, Thr,[63,64] or water. A sequential or concerted series of such elementary transfer events may ultimately deliver a proton taken up from the solvent into the active site or from one side of a membrane-spanning proton pump to the other side.[3] The steps of protonation and deprotonation may be associated with conformational changes in the protein structure that bring the proton-exchanging groups in close proximity. In transient protonation and deprotonation events, side-chain motion may carry a proton from one region to another, as has been proposed for cytochrome *c* oxidase.[28,30,35] Side-chain motion may also transiently lead to simultaneous hydrogen bond acceptance and donation of a nonionizable but proton-conducting group, such as the hydroxyl group of Thr, to form a transient Grotthuss proton relay. In the method presented here, we first identify possible proton pathways in the static structure and then extend them by incorporating dynamic fluctuations of side chains and water.

We start by constructing proton-conducting networks based on a molecular structure of the protein obtained, for example, from X-ray crystallography or nuclear magnetic resonance spectroscopy. As input information, we use the positions of heavy atoms such as oxygen, nitrogen, and sulfur that can participate in proton transfer, as listed in Table 1. In the simplest model, the coordinates of hydrogen atoms are not included. In the next step, all possible pairs of protein atoms, as listed in Table 1, are examined. A pair of donor and acceptor atoms within a clustering distance d is considered to be part of the same cluster. Therefore, any member of a given cluster is directly or indirectly connected to all other members of the cluster. The clustering distance $d = 3.5$ Å is chosen to be larger

(50) Cupp-Vickery, J. R.; Poulos, T. L. *Nat. Struct. Biol.* **1995**, *2*, 144.
(51) Di Primo, C.; Hui Bon Hoa, G.; Douzou, P.; Sligar, S. *J. Biol. Chem.* **1990**, *265*, 5361.
(52) Vidakovic, M.; Sligar, S. G.; Li, H. Y.; Poulos, T. L. *Biochemistry* **1998**, *37*, 9211.
(53) Gerber, N. C.; Sligar, S. G. *J. Biol. Chem.* **1994**, *269*, 4260.
(54) Shimada, H.; Makino, R.; Imai, M.; Horiuchi, T.; Ishimura, Y. *International Symposium on Oxygenases and Oxygen Activation*; Yamada Science Foundation: Osaka, Japan, 1990; pp 133−136.
(55) Gerber, N. C.; Sligar, S. G. *J. Am. Chem. Soc.* **1992**, *114*, 8742.
(56) Benson, D. E.; Suslick, K. S.; Sligar, S. G. *Biochemistry* **1997**, *36*, 5104.
(57) Imai, M.; Shimada, H.; Watanabe, Y.; Matsushi-Mahibiya, Y.; Makino, R.; Koga, H.; Horiuchi, T.; Ishimura, Y. *Proc. Natl. Acad. Sci. U.S.A.* **1989**, *86*, 7823.
(58) Martinis, S. A.; Atkins, W. M.; Stayton, P. S.; Sligar, S. G. *J. Am. Chem. Soc.* **1989**, *111*, 9252.
(59) Hishiki, T.; Shimada, H.; Nagano, S.; Egawa, T.; Kanamori, Y.; Makino, R.; Park, S. Y.; Adachi, S.; Shiro, Y.; Ishimura, Y. *J. Biochem.* **2000**, *128*, 965.
(60) Harris, D. L.; Loew, G. H. *J. Am. Chem. Soc.* **1994**, *116*, 11671.
(61) Kimata, Y.; Shimada, H.; Hirose, T.; Ishimura, Y. *Biochem. Biophys. Res. Commun.* **1995**, *208*, 96.
(62) Raag, R.; Martinis, S. A.; Sligar, S. G.; Poulos, T. L. *Biochemistry* **1991**, *30*, 11420.
(63) Liepinsh, E.; Otting, G. *Magn. Reson. Med.* **1996**, *35*, 30.
(64) Wüthrich, K. *NMR of Proteins and Nucleic Acids*; Wiley: New York, 1986.

Table 1. Donor and Acceptor Atoms in Proton Transfer Networks

residue	atom
ASP	OD1, OD2
GLU	OE1, OE2
HIS	ND1, NE2
CYS	SG
TYR	OH
SER	OG
THR	OG1
ARG	NH1, NH2, NE
HOH	O
HEM	O1A, O2A, O1D, O2D

than a typical hydrogen bonding distance of about 3 Å to account for molecular flexibility and dynamic effects. Alternatively, one would use the algorithm with a shorter d (~3 Å) to analyze an *ensemble* of conformations obtained from molecular dynamics simulations. This procedure provides us with an extensive list of clusters of varying sizes that may then be used to locate the possible pathways. For example, all pathways leading to the distal oxygen atom in the cytochrome P450cam structure are contained in the cluster in which the distal oxygen is present. This procedure generally yields an extensive set of potential pathways corresponding to the static structure of the protein. However, most of these pathways are fragmented and do not extend, for example, from the surface of the protein into a buried active site.

Conformational and Hydration Fluctuations. The network analysis of the static structure may miss critical links between fragmented parts of the hydrogen bond network. Dependent on the resolution of the protein structure, difficulties may arise in particular when (i) the water molecules and side chains involved in proton transfer are relatively mobile or (ii) alternate side-chain positions have low occupancies ($\leq$0.3). To bridge the resulting gaps, we carry out an extensive search of the conformational space of the side-chain rotamers. For this purpose, the dihedral angles of side chains of selected groups are varied by rigid body rotation, keeping bond distances and angles constant. Note that, for the amino acid residues listed in Table 1, the number of side-chain dihedral angles that may be varied independently ranges from 1 (e.g., Thr) to 5 (Arg). Each dihedral angle is varied on a grid from 0° to 360°. Therefore, for the side-chain rotation of n groups with m_i dihedral angles each ($i = 1,.., n$), we sample an $M(=\sum_{i=1,n} m_i)$-dimensional conformational space with a flexible grid length in each dimension.

To determine the relative weights of rotated structures, we estimate their conformational energies. At the simplest level, the dominant contributions to this energy are derived from steric interactions, approximated here by a soft-sphere model. The potentials between pairs of heavy atoms i and j are described by

$$u(r_{ij}) = k_B T\left(\frac{R_i + R_j - 2\delta}{r_{ij}}\right)^{12}, \qquad (1)$$

where r_{ij} is their distance, R_i and R_j are their van der Waals radii (as compiled in Table 2), and $\beta^{-1} = k_B T$, where k_B is Boltzmann's constant and T is the temperature. In our simplified approach, we have not directly taken into account protein-backbone motion which effectively softens the side-chain interactions. Instead, we reduce each van der Waals radius by a small amount, $\delta = 0.2$ Å. This corresponds to about half of the positional fluctuations of atoms with a crystallographic B-factor of about 10 Å^2, which is typical of well-resolved protein structures.

Table 2. Van der Waals Radii R_i

atom	radius (Å)
C	1.90
N	1.50
O	1.40
S	1.85
FE	0.64

A neighbor list is enumerated for each atom belonging to the fluctuating side chains, and then the energy of a given structure evaluated by summing up all pair interactions. In this step, we include full 1−4 interactions within a given residue, but no explicit single-bond torsion-angle potential was assumed. Comparison with the energy of the static structure gives the energy cost, ΔE_k, to obtain the k-th structure (with one or more side chains rotated through given angles).

To address the involvement of mobile water molecules, we use the potential-of-mean-force (PMF) method[33,65,66] for studying the internal hydration of the structures, rotated or unrotated. This method is based on a statistical mechanical expression for the water-density distribution in terms of particle correlation functions. In the PMF calculations, only the positions of the heavy atoms of the protein are considered, without including information about crystallographic water sites. The simplicity and computational speed of the PMF calculations allow us to estimate changes in the hydration structure as side chains are rotated from their resting positions. Inclusion of conformational and hydration fluctuations therefore provides us with an ensemble of structures that we analyze in terms of networked clusters to identify potential pathways for proton translocation from the surface to the active site.

Connectivity Matrix. Side-chain rotations may lead to changes in the hydrogen bond connectivity. Here, we are primarily interested in finding new connections between pairs of proton-conducting residues. We define an energy-weighted connectivity matrix:

$$P_{ij} = \frac{\sum_k e^{-\beta \Delta E_k} f_{ij}^k}{\sum_k e^{-\beta \Delta E_k}} \qquad (2)$$

where P_{ij} refers to the probability of establishing a connectivity between atoms i and j. The summation in the right-hand side of eq 2 runs over all structures in the ensemble. f_{ij}^k is the connectivity parameter, with $f_{ij}^k = 1$ if the distance between the atoms i and j in the k-th structure is less than a cutoff distance, $d_{max} = 3.5$ Å, and $f_{ij}^k = 0$ otherwise.

Best-Path Analysis. After the identification of possible proton-transfer networks, we investigate their kinetic relevance. Within the present framework, this requires the analysis of pathways on an M-dimensional energy hypersurface. This is a formidable task when M is large. We employ Dijkstra's

(65) Hummer, G.; Soumpasis, D. M. *Phys. Rev. E* **1994**, *50*, 5085.
(66) Hummer, G.; Garcıa, A. E.; Soumpasis, D. M. *Biophys. J.* **1995**, *68*, 1639.

algorithm[67] to find an "optimal" path between two conformations. The conformational space is represented as vertices on an M-dimensional periodic grid, with each dimension corresponding to one of the rotated dihedral angles. We assume that transitions occur only between adjacent vertices and approximate the transition probability between such vertices i and j by

$$p(i \rightarrow j) = \min\{1, \exp[-\beta \Delta E(ij)]\} \qquad (3)$$

where $\Delta E(ij) = \Delta E_j - \Delta E_i$ is the energy difference between the two vertices i and j. The transition rate along a path of mutually adjacent vertices is then approximated by

$$p(i_0 \rightarrow i_1 \rightarrow \ldots \rightarrow i_N) = \prod_{\alpha=0}^{N-1} p(i_\alpha \rightarrow i_{\alpha+1}) \equiv \mathrm{e}^{-S} \qquad (4)$$

where the "action" S is the sum of the energy increases of all uphill steps. We have also performed path optimizations using a refined action with probabilities $p(i \rightarrow j) = \exp[-\beta \Delta E(ij)]/\sum_k \exp[-\beta \Delta E(ik)]$, where the sum extends over neighbors k of vertex i. This does not change the results significantly.

Dijkstra's algorithm[67] allows us to find the "best path" between any two conformations by searching for the path with the minimum action S (i.e., with the smallest sum of uphill energy increments). Using this best-path analysis, one can subsequently identify a "transition state" and an "activation energy" required for the passage of the system from its initial resting structure to one in which a desired connectivity has been established. Dijkstra's algorithm can also be used to find the n best paths by searching the directed graph of all paths and truncating that search based on the known optimal path from any intermediate vertex to the final vertex. As the dimension M increases, searching for the optimal paths becomes computationally costly, and alternative methods such as transition path sampling[68] can be used instead.

In summary, starting from the static structure, we generate an ensemble of structures by rotating sequentially the side chains of proton-conducting residues. An energy-weighted connectivity matrix is constructed. With a given connectivity threshold $P_{ij} > P_{\min}$, proton-conducting residues are clustered to identify dynamically added proton connectivities. From this clustering, one can determine above which threshold the active site is connected to the solvent and which groups are involved. From a best-path analysis, one can then estimate a path in the space of side-chain dihedral angles and the steric energy along that path. This provides a crude estimate of a conformational activation energy which can be used to distinguish between different models of proton transfer.

Results and Discussion: Application to Cytochrome P450cam

In the following, we apply the network model to proton transfer in cytochrome P450cam based on a recent high-resolution structure with a molecular dioxygen bound to the heme iron (PDB code: 1dz8, A chain).[47] We first examine the connectivities of the distal oxygen atom in the static structure, as shown in Figure 1. It is found that both Thr-252 and water 901 are connected to the distal oxygen as parts of a small cluster comprised otherwise of bound water molecules. This cluster terminates on Glu-366, which is not connected to the protein surface.[52] Thus, there is no direct proton access to the heme-bound dioxygen if only the static structure is considered. The heme hydration cluster[33] forms the largest network in the static structure and provides a possible proton path into the substrate binding site. However, with the bound camphor substrate blocking the path, a connection to the distal oxygen would require considerable substrate motion. Asp-251, suggested as a possible proton entry site,[54,55] is found to be extensively connected to the protein surface via residues Lys-178, Asp-182, Thr-185, Arg-186, and water 149. But, as shown in Figure 1, the side-chain oxygen atoms of Asp-251 point away from the heme and there is no apparent link between the clusters containing Asp-251 and the distal oxygen O_2-418.

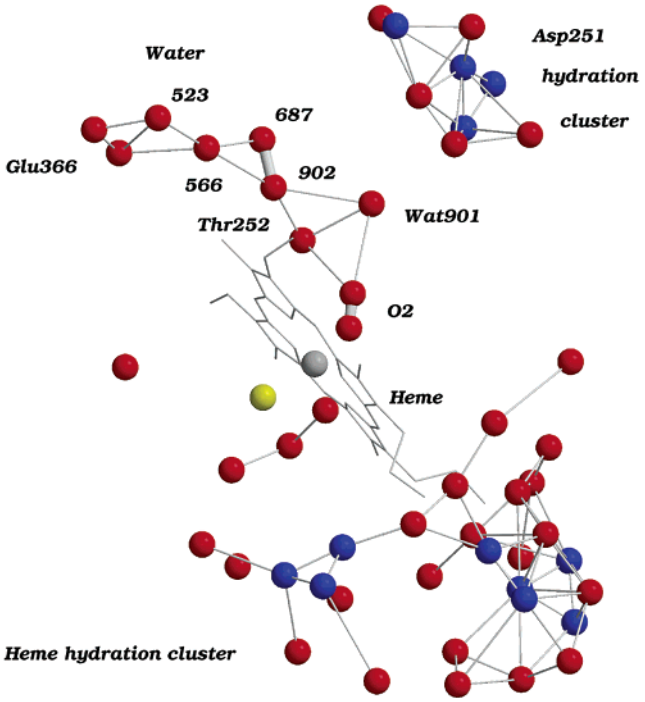

Figure 1. Connectivity of the distal oxygen in the static structure of P450cam (PDB code 1dz8[47]). Donor and acceptor atoms within 3.5 Å are connected by lines, with three large proton-transfer networks formed near the active site. The cluster containing the dioxygen is shown at the top center above the heme. The Asp-251 cluster is at the top right. Parts of the heme propionate cluster are shown at the bottom right. Oxygen, nitrogen, and sulfur atoms are shown in red, blue, and yellow, respectively. The heme is shown in gray. Molscript is used for molecular graphics.[77]

The static structure does not reveal a well-defined proton pathway to the distal oxygen. Protein and water motions thus appear essential for proton delivery into the active site of P450cam. We next examine the role of side-chain conformational fluctuations in the formation of functional proton pathways. We first compile a list of 285 possible proton donor and acceptor atoms in 161 amino acid residues with polar side chains and the dioxygen ligand based on the PDB protein structure 1dz8[47] and the atoms listed in Table 1. We extensively sample conformation space by rotating the dihedral angles of each side chain, while keeping all other side chains in their respective crystallographic orientation, and without considering crystallographic water molecules. A Boltzmann-weighted connectivity matrix is constructed based on eq 2. Conformations are sampled at angle increments of 5°, except for Lys (10°) and Arg (20°), which were appropriately reweighted in eq 2.

(67) Dijkstra, E. W. *Numer. Math.* **1959**, *1*, 269.
(68) Dellago, C.; Bolhuis, P. G.; Chandler, D. *J. Chem. Phys.* **1998**, *108*, 9236.

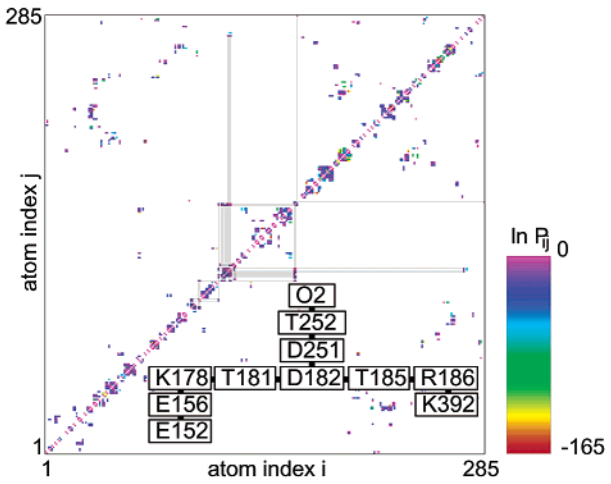

Figure 2. Connectivity matrix P_{ij} in cytochrome P450cam with side-chain rotations but excluding water molecules. The *x* and *y* axes correspond to the atom indices *i* and *j* in a list of 285 donor and acceptor atoms, ranked as in the PDB structure 1dz8.[47] The color coding of the connectivities is based on ln P_{ij}, with the strongest connections (ln $P_{ij} \approx 0$) shown in purple and the weakest (ln $P_{ij} \approx -165$), in red. The extent of the network containing the dioxygen molecule is shown with thin black lines that connect atom pairs *ij* and *ik* of the dioxygen cluster if P_{ik} or $P_{jk} > 10^{-14}$. The inset in the lower half traces the connectivity from the dioxygen to residues at or near the protein surface.

A two-dimensional representation of the resulting connectivity matrix is shown in Figure 2. The *x* and *y* axes correspond to the indices of the donor and acceptor atoms in the atom list. Connectivities P_{ij} between atoms *i* and *j* are shown as color coded points at positions (*i*, *j*). We clustered the donor and acceptor atoms based on pair connectivities. Atoms *i* and *j* are assumed to be connected if $P_{ij} > 10^{-14}$. In Figure 2, the cluster containing the distal oxygen has been highlighted by joining directly connected atoms with vertical and horizontal lines. Note that the pathways resulting from this cluster can thus be traced out by following the lines. An exhaustive sampling of single amino acid and dioxygen rotations puts the distal oxygen into a cluster of 23 proton-conducting groups (belonging to residues 152−156, 178−182, 185−186, 188, 190, 251−252, and 392) based on a probability threshold of $P_{ij} > 10^{-14}$, and without including water. In particular, dynamic side-chain fluctuations establish a weak connection between the distal oxygen and Asp-251 at a threshold of 4×10^{-14}. With crystallographic water included, the size of the dioxygen cluster increases to 506 atoms at that threshold.

The connectivity matrices reveal alternative proton pathways from the protein surface to the active site. Without crystallographic water, a single pathway through Thr-252 connects the distal oxygen of the dioxygen ligand to Asp-251 at the protein surface. With crystallographic water, this pathway is again present and water-901 bridges between Thr-252 and Asp-251. An additional pathway connects the dioxygen through Thr-252 and water 902 to Glu-366 and water 523, neither of which are connected to the surface in the static crystallographic structure. So only pathways through Asp-251 appear viable for proton transfer into the active site. Protonation of Asp-251 can occur directly from the solvent or through one of the neighboring residues (Lys-178, Asp-182, and Arg-186) with which Asp-251 forms the charge cluster.

We will next investigate in more detail possible proton-delivery mechanisms involving Asp-251 as a shuttle connecting the protein surface to the active site. In the static structure, Asp-251 is directed toward the surface, with a distance of about 9 Å between OD1 and the distal oxygen. As discussed previously, rotation can bring the side chain of Asp-251 pointing toward the heme. But the low value of P_{ij} suggests that a direct connection is unlikely. However, with Asp-251 in a rotated state, the internal water molecule 901 may help establish a protonic connection to the distal oxygen. Water 901 was first observed in a recent high-resolution, low-temperature crystal structure of functional intermediates[47] and was not detected in earlier crystallographic studies of P450cam. Interestingly, the structure of a P450 complex with the inhibitor 2-phenyl imidazole[69] indicated the presence of a water molecule (labeled as water 720, PDB code 2cp4) similarly located in this region. Nevertheless, water 720 in 2cp4 is not directly connected to Thr-252 (at a distance of 5.81 Å from the side chain oxygen), whereas water 901 in 1dz8 is at a hydrogen bonding distance of 2.98 Å. PMF hydration calculations using the PDB structure 5cp4[52] of the camphor-bound enzyme also indicate a low density hydration site at a position overlapping with the carboxylic acid group of the rotated Asp-251 but displaced slightly with respect to water 901 in 1dz8 because of a substantial shift in the Thr-252 conformation. Schlichting et al.[47] pointed out that a deformation of the backbone involving the carbonyl oxygen of Asp-251 and the amide nitrogen of Thr-252 appears to stabilize water 901 in the "groove" of the distal I helix. Clearly, water 901 is potentially relevant for proton delivery into the active site in conjunction with Asp-251 side-chain rotation and possible interactions with Thr-252.

Based on the preceding analysis, we now focus our search onto the region of Asp-251 for pathways extending into the active site. In particular, we explore the role of Asp-251 as a proton shuttle in four different models with increasingly detailed descriptions of the local hydration structure.

Table 3. Dihedral Angles of Asp-251, Thr-252, and O2-418 in the Crystal Structure 1dz8[47] and Models 1−4[a]

	Asp-251		Thr-252	O_2-418
model	χ_1	χ_2	χ_T	χ_0
1dz8-A	−152.0	29.2	52.5	151.1
1	53.0	39.2	32.5	121.1
2	3.0	114.2		
3	3.0	−60.8		
4	−47.0	109.2		

[a] Asp-251: $\chi_1 \equiv$ N−CA−CB−CG, $\chi_2 \equiv$ CA−CB−CG−OD1. Thr-252: $\chi_T \equiv$ N−CA−CB−OG1; $\chi_0 \equiv$ NA(HEM-417)−FE(HEM-417)−O1−O2, where the latter two atoms belong to the ligand O_2.

Model 1: Asp-251 Proton Shuttle without Water. In the first model, crystallographic water molecules near the active site are excluded. Simultaneous rotation of the four dihedral angles of Asp-251, Thr-252, and O_2-418 leads to close connections between the three groups. The dihedral angles in a sterically optimal networked structure are listed in Table 3. The steric energy favors the rotated structure relative to the crystal structure by about $-0.2\ k_BT$, but inclusion of electrostatic energies (arising, e.g., from protonation of Asp-251 and disruption of the charge cluster around it) would certainly shift this value. Nevertheless, the rotated side chain of Asp-251 fits nicely into a small cavity near Thr-252. In the sterically optimal structure, the distance between OD1 of Asp-251 and OG1 of

(69) Poulos, T. L.; Howard, A. J. *Biochemistry* **1987**, *26*, 8165.

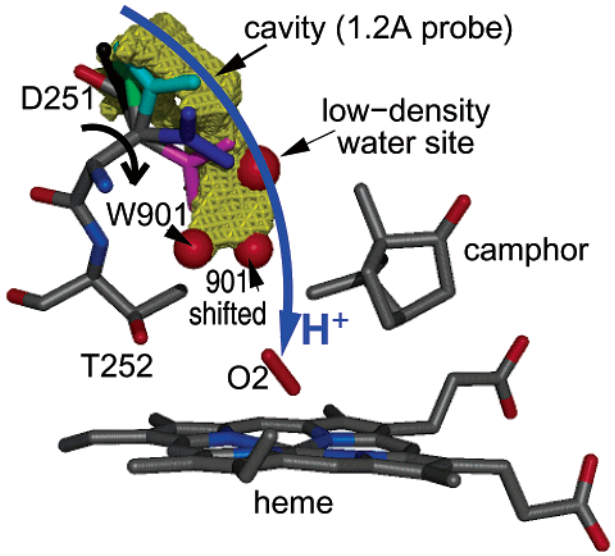

Figure 3. Side-chain rotation of Asp-251. Several snapshots of the Asp-251 side chain along the optimal path into the active site are shown. Water 901 of 1dz8,[47] the shifted water 901 site, and an additional low-density water site are shown as red spheres. Shown in yellow is the extent of the internal cavity that contains the water sites, and through which the Asp-251 side chain slides. The cavity was calculated for a spherical probe of radius 1.2 Å and protein atom radii as in Table 2, without considering the side chain of Asp-251. The blue arrow indicates the direction of the proton relay (molecular graphics prepared with MidasPlus[78]).

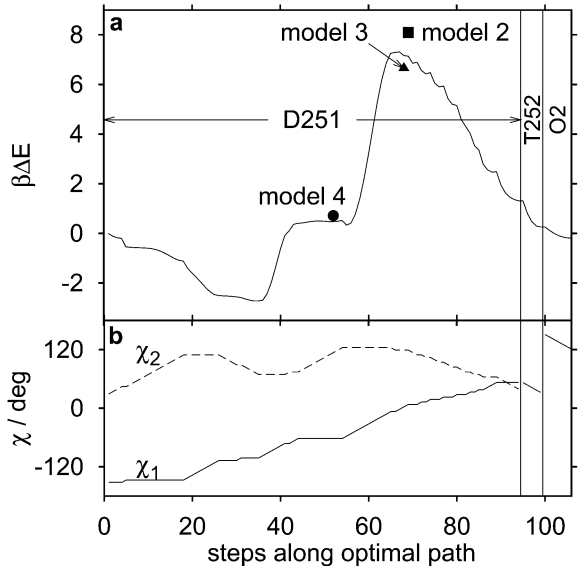

Figure 4. Energetics of the sterically optimal path of proton delivery to the distal oxygen. (a) The difference in steric energy from the resting structure along the optimal path of model 1 is shown as a solid line. Horizontal arrows indicate the range of Asp-251 rotation (steps 1−94). Vertical lines indicate the range of Thr-252 and dioxygen rotation (steps 95−99 and 100−106, respectively). The end points of the paths of models 2−4 are shown as filled symbols. (b) Side-chain dihedral angles along the optimal path of model 1 for Asp-251, Thr-252, and the dioxygen molecule. The Asp-251 side chain follows similar paths in models 2 and 4.

Thr-252 is found to be about 3.2 Å, and the distance between OG1 and O2 is 3.1 Å. The distance between OG1 and O2 is below 3.5 Å in 87% of the Boltzmann-weighted structures (i.e., $P_{ij} = 0.87$). In contrast, the corresponding probability of getting a network connection between Asp and Thr is merely 2.1% if all three residues are rotated simultaneously.

The rotation of the Thr-252 side chain is found to be relatively unhindered even in the presence of water 901. As the side-chain dihedral angle, χ_T changes from 52.46° in the static structure to values close to 0°, the steric energy changes are small (about $1k_BT$). The motion of O_2-418 is also largely free of steric barriers. Only the rotation of Asp-251 encounters a substantial steric barrier in the formation of a hydrogen bond network between Asp-251, Thr-252, and the distal oxygen. As the side chain of Asp-251 is rotated from the protein surface into the interior, it passes through a tight channel, as shown in Figure 3. The extent of the cavity was determined by placing a spherical probe atom of radius 1.2 Å onto a Cartesian grid of 0.25 Å width, with protein atom radii as in Table 2 and the Asp-251 side-chain atoms excluded. Motion of the Asp-251 side chain is hindered mainly by its amide group and the carbonyl oxygen of Val-247. The steric activation energy required to rotate Asp-251 into the active-site region is estimated to be about $10k_BT$, based on the optimal path starting from the static structure (Figure 4). Along that path, the "transition state" of Asp-251 rotation occurs at $\chi_1 = -2.0°$ and $\chi_2 = 119.2°$.

The dynamics of the protein matrix may somewhat soften these steric interactions. However, conformational isomerization of the side chain past the backbone ($\chi_1 \approx 0$) ensures that a substantial barrier persists. Nevertheless, even in the absence of intervening water molecules, proton transfer from the surface to the distal oxygen seems feasible entirely via conformational fluctuations of amino acid side chains. However, at the "transition state" (i.e., at the top of the steric energy barrier along the "best path"), OD1 of Asp-251 is already within 2.8 Å of the crystallographic site of water 901. This strongly suggests the participation of water 901 in proton delivery, as explored next.

Model 2: Asp-251 Proton Shuttle with Crystallographic Water. Internal water molecules are expected to facilitate long-range proton transfer in proteins. We consider the crystallographic water molecules associated with the A chain in 1dz8.[47] In the energetic analysis, the water molecules are assumed to be fixed at their crystallographic positions. Rotation of Asp-251 along the same path as before again establishes a protonic connection into the active site, now through water 901 which is located 3.5 Å from the distal oxygen. Water 901 is contained in the cavity traced out by the rotated side chain of Asp-251 of model 1, and it blocks a direct connection between Asp-251 and Thr-252, as shown in Figure 3. The steric energy at the endpoint of the optimal path for Asp-251 rotation in the presence of water is shown in Figure 4, corresponding to Asp-251 dihedral angles of $\chi_1 = 3.0°$ and $\chi_2 = 114.2°$ and a distance of $d_{WD} = 2.64$ Å between OD1 and water 901 (Table 3). The initial part of the path is downhill in steric energy until it reaches the configuration with $\chi_1 = -102.04°$ and $\chi_2 = 79.22°$ and $d_{WD} = 5.4$ Å. From there on, Asp-251 encounters the same steric activation barrier as in model 1, as it slides past its own backbone before forming a connection to water 901. Water 901, while on the proton path into the active site, thus does not by itself lower the steric activation barrier for Asp-251 conformational isomerization. Moreover, at a distance of 3.5 Å, a constrained water 901 does not seem capable of delivering the proton directly to the distal oxygen.[47]

Model 3: Motion of Water 901 and Asp-251. We will next explore the role of water 901 motion in mediating proton transfer from Asp-251 to the heme-bound dioxygen. Water 901 is the most likely candidate for protonation of the distal oxygen if

the OH group of Thr-252 is not directly involved, as concluded from mutation experiments.[61] Therefore, we examine the hydration structure in the region of water 901 by a PMF hydration calculation on a 0.25 Å grid. This calculation reproduces the water 901 site nicely, with a water-density peak of about 30 times bulk density ρ_0 within 0.4 Å. Such a high calculated water density is typical of crystallographic sites.[33] Interestingly, the density profile, while peaked near water 901, extends for about 1.7 Å toward the camphor substrate and the distal oxygen. This is also supported by the cavity search shown in Figure 3, with water 901 and its shifted site at the border of the cavity defined by a 1.2 Å probe. From these results, we conclude that, on average, water 901 resides at the crystallographic position but can move toward the active site.

Within a contour level of $\rho = 4\rho_0$ of calculated water density, water 901 can establish a hydrogen bond with the distal oxygen at an O−O distance of 2.9 Å. In that shifted position, water 901 loses its hydrogen bond to the OH of Thr-252 (3.85 Å O−O distance). However, as a prerequisite for proton delivery into the active site, the shifted water 901 is capable of simultaneously donating a hydrogen bond to the distal oxygen and accepting a hydrogen bond from a protonated and rotated Asp-251. Its second hydrogen can remain hydrogen bonded to the carbonyl oxygen of Val-247 at an O−O distance of 3.0 Å and an almost ideally tetrahedral angle of 116° between the distal oxygen. In summary, the motion of water 901 toward the dioxygen appears feasible based on a PMF hydration calculation and results in a hydrogen bonding geometry suitable for proton delivery in conjunction with Asp-251 conformational isomerization.

For an Asp-251 side-chain orientation of $\chi_1 = 3.0°$ and $\chi_2 = -60.8°$, the distance between OD2 and the shifted water 901 site is $d_{WD}' \approx 2.7$ Å. In a best-path analysis of Asp-251 rotation starting from the resting structure, the hydrogen bond connection is found to occur at the "transition state", as defined by the steric energy barrier. In conclusion, a high steric activation barrier persists even if OD1 of Asp-251 is brought within 3 Å of the shifted water 901.

Model 4: Two-Water Mediated Asp-251 Shuttle. Measurements of kinetic isotope effects and their interpretation within a proton inventory analysis[52] indicated the possible involvement of at least two water molecules in the proton delivery mechanism of P450cam. A PMF hydration calculation indeed shows a second low-density hydration site between water 901 and Asp-251. This site is shown in Figure 3. In the resting structure, the calculated water density at this site is just above noise (2.9 times bulk density). But, as Asp-251 is rotated along the sterically optimal path, the calculated density at that site increases to 5.2 times the bulk density. Whereas this is considerably lower than densities seen at crystallographic water sites,[33] it nevertheless suggests the possible transient presence of a water molecule.

A comparatively small motion of Asp-251 from its resting state to a conformation with side-chain dihedral angles of $\chi_1 = -47.0°$ and $\chi_2 = 109.2°$ brings OD1 of Asp-251 to a distance of 2.79 Å from this low-density hydration site (Table 3), which in turn is at a distance of 2.76 Å from the water 901 site. In this rotated state, a network comprised of 63 proton donor and acceptor atoms connects the protein surface to the distal oxygen via Asp-251, the low-density water site, and water 901. Conformational isomerization of Asp-251 into a bridging configuration between the active site and the protein surface requires breaking of the hydrogen bonds of the charge cluster formed by Lys-178, Asp-182, Thr-185, and Arg-186. However, as shown in Figure 4, the endpoint of the sterically optimal path is reached before the Asp-251 side chain slides past the protein backbone, and thus, no substantial steric barrier is encountered in the rotation.

During the initial proton uptake, the solvent-exposed oxygen of Asp-251 appears more likely to become protonated, with surface water 149 within 3.66 Å in 1dz8.[47] A transiently neutralized Asp-251 might sufficiently destabilize the charge cluster containing Lys-178, Asp-182, Arg-186, and Asp-251 to trigger Asp-251 conformational isomerization. We find that, initially, conformational isomerization is sterically favorable by about $-2.5k_BT$ (i.e., there is sufficient space for the carboxylic group to rotate the χ_2 dihedral angle) and maintains the hydrogen bond between the second, unprotonated carboxylic oxygen and NH1 of Arg-186. A further rotation of Asp-251, sterically uphill by about $3.4k_BT$ from the minimum along the path, establishes the bridging configuration. In this configuration, a protonated oxygen OD1 is closest to the low-density water site, facilitating a subsequent proton transfer into the active site via this transiently occupied water site and water 901.

Conclusions

Network models provide a simple yet useful basis for probing the structure−function relationship in biomolecular proton transfer.[17−19] Under the assumption of a Grotthuss-like charge relay mechanism, protons are translocated via hydrogen bonded networks of polar amino acid side chains and bound water molecules. Here, we have developed a general method to locate such proton-conducting pathways in proteins of known structure. We find that proton-transfer networks are often fragmented if the static structure alone is considered. Fluctuations in the protein conformation and hydration structure are thus essential for functional proton delivery pathways. We have shown how side-chain conformational fluctuations coupled to dynamic alterations in the hydration structure connect a deeply buried proton acceptor to the solvent-exposed surface of a protein.

Several simplifying assumptions permit an extensive sampling of the protein conformational fluctuations. First, only the steric interactions of the fluctuating side chains with the surrounding protein matrix are considered. Whereas this may account for a dominant part of the activation barrier, actual reaction paths may derive significant contributions from other interactions such as those involving charges. Second, the present treatment employs a grid method to vary the dihedral angles. Alternative methods can be used within the same framework, such as random sampling of dihedral angles, possibly combined with importance sampling. Third, backbone dynamics of the protein and global motions are neglected but may play a significant role, as illustrated in P450cam by a partially broken helix.[47] Fourth, we assume that the hydration can be treated within the PMF framework, which in turn assumes that the water structure is in equilibrium as the side chains are rotated. While being approximate, the PMF method points to possible hydration sites that can subsequently be explored in detail by experimental (e.g., site-directed mutagenesis) or additional theoretical means (e.g., molecular dynamics simulations).

Identification of a sterically optimal path for proton delivery via side-chain rotation is an important element in the quantitative

description of long-range biomolecular proton transfer. Here, we used Dijkstra's algorithm to identify the energetic saddle points and optimal paths on the energy surfaces spanned by the side-chain dihedral angles, based on a simple path action. This method performs efficiently for low-dimensional systems (i.e., simultaneous rotation of few dihedral angles). Alternatively, a high-dimensional energy surface could be searched, for example, by generating an ensemble of transition paths.[68]

In cytochrome P450cam, the static structure reveals several fragmented proton pathways but no direct connection from the protein surface to the active site. We show that side-chain motion and water molecules can establish such pathways connecting a solvent-exposed cluster of charged amino acids to the heme-bound dioxygen. In those pathways, the highly conserved Asp-251 acts as a proton shuttle by providing a crucial network connection through side-chain rotation, as has been suggested by Gerber and Sligar.[55] Motion of a protonated Asp-251 side chain toward the heme is sterically feasible because of a narrow cavity extending to an interior water site (901 in 1dz8[47]). Direct transfer of the proton from a rotated Asp-251 to the distal oxygen is not possible without major structural rearrangements and, thus, should involve intermediate groups. Whereas Thr-252 bordering the active site cavity is, in principle, capable of bridging between a rotated Asp-251 and a heme-bound dioxygen, we find that this involves a high steric activation energy. Indeed, mutation data do not suggest a direct participation of Thr-252 in a charge relay.[61] Instead, we find that internal water molecules could facilitate proton transfer. In particular, an important bridging role is played by water 901, recently identified near the active site in a functional intermediate,[47] but not seen in earlier structures. A PMF calculation shows that its hydration site is elongated, and after a small displacement (1.7 Å), it can form tight hydrogen bonds simultaneously with a rotated Asp-251 side chain and the distal oxygen. However, to establish such a charge relay, the side chain of Asp-251 is required to slide tightly past the protein backbone, resulting in a significant steric activation barrier. Alternatively, a vacant water site between Asp-251 and water 901 can be transiently occupied by a water molecule diffusing in from the nearby solvent. This would not only eliminate much of the steric activation energy but could also explain the involvement of multiple water molecules deduced from an experimental study of proton kinetic isotope effects.[52]

Penetration of water molecules into the substrate region was indeed observed in a crystal structure of P450cam for a substrate with a long tail extending into the solvent.[70] Transient water penetration into the interior of cytochrome *c* was observed in molecular dynamics simulations.[42] In a recent study of water penetration into hydrophobic channels,[40,41] it was found that small increases in the local polarity can be sufficient to fill a previously empty cavity by water. In P450cam, a polarity increase appears to be triggered by dioxygen binding to the heme. The resulting backbone rearrangement exposes the amide hydrogen of Thr-252 to a narrow cavity that becomes filled with water 901.[47] Facile proton access is thus possible in the intermediate but not without water 901. This could be relevant to prevent uncontrolled proton delivery into the active site and uncoupling.

This simple mechanism can also be used to rationalize the results of Asp-251 mutations. Replacing Asp-251 by Asn results in a substantial slowdown of camphor hydroxylation but not a complete loss of activity.[52,54−56] Sampling of side-chain rotamers of the Asp-251-Asn mutant, with water molecules included at the crystallographic positions (PDB code: 6cp4[52]), does not yield a proton shuttle into the active site equivalent to that of Asp-251. Alternatively, proton access from the solvent could be provided by a water chain involving the low-density water site found here, together with water 901 (1dz8[47]) and additional water molecules. Water-mediated proton transfer has indeed been proposed based on the large kinetic isotope effect in the Asp-251-Asn mutant compared to wild-type P450cam.[52]

We have also explored a mutation of Asp-251 to Glu. One might expect that the longer side chain could facilitate direct proton shuttling to Thr-252 without intervening water molecules. However, dihedral angle rotations of the Glu-251 side chain result in steric barriers higher than those encountered by Asp-251 (models 1 and 2), even with water 901 included in the proton relay (model 3). As in the unmutated enzyme (model 4), the additional low-density water site largely eliminates the steric barriers required for proton transfer. Ignoring the possibility of substantial rearrangements in the intricately balanced charge cluster formed with Lys-178, Asp-182, and Arg-186, we conclude from this that Asp251Glu could be competitive with the wild-type enzyme only if a second water molecule mediated the proton transfer.

Molecular dynamics simulations could provide us with detailed descriptions of the formation and dynamics of such pathways up to the nanosecond time scale.[71−74] However, the formation of a complete proton-transfer pathway is expected to be a rare event in many cases, occurring on time scales longer than those amenable to current fully atomistic simulations. If a suitable reaction coordinate is known, such barrier-crossing events can be enhanced by biased dynamics. The identification of potential proton-conducting pathways is thus a crucial element not only in designing experiments but also in the implementation of computationally efficient molecular simulations. This is illustrated, for example, by studies of proton transfer in cytochrome *c* oxidase utilizing Glu-242 rotation.[28,30,35]

The kinetic relevance of pathways has been estimated from steric interactions alone. Inclusion of charge effects in the present framework is possible, in principle, but would require precise estimates of the amino acid protonation states[5,13−16] and an accurate modeling of the dielectric environment of the protein interior in the presence of mobile water molecules and amino acid side chains.[75,76]

Even with accurate conformational energies, the kinetic analysis of long-range proton transfer in proteins is nontrivial. For example, in understanding the role of Asp-251 as a proton shuttle, one may have to consider several steps such as breaking

(70) Dmochowski, I. J.; Crane, B. R.; Wilker, J. J.; Winkler, J. R.; Gray, H. B. *Proc. Natl. Acad. Sci. U.S.A.* **1999**, *96*, 12987.
(71) Lu, D. S.; Voth, G. A. *Proteins: Struct., Funct., Genet.* **1998**, *33*, 119.
(72) Brewer, M. L.; Schmitt, U. W.; Voth, G. A. *Biophys. J.* **2001**, *80*, 1691.
(73) Baudry, J.; Tajkhorshid, E.; Molnar, F.; Phillips, J.; Schulten, K. *J. Phys. Chem. B* **2001**, *105*, 905.
(74) Chen, K. S.; Hirst, J.; Camba, R.; Bonagura, C. A.; Stout, C. D.; Burgess, B. K.; Armstrong, F. A. *Nature* **2000**, *407*, 110.
(75) Simonson, T.; Archontis, G.; Karplus, M. *J. Phys. Chem. B* **1999**, *103*, 6142.
(76) Dillet, V.; Van Etten, R. L.; Bashford, D. *J. Phys. Chem. B* **2000**, *104*, 11321.
(77) Kraulis, P. J. *J. Appl. Crystallogr.* **1991**, *24*, 946.
(78) Ferrin, T. E.; Huang, C. C.; Jarvis, L. E.; Langridge, R. *J. Mol. Graphics* **1988**, *6*, 13.

of the hydrogen bond network stabilizing Asp-251 in its crystallographic position, protonation of Asp, fluctuation of the Asp side chain, deprotonation of Asp, and the transfer of the proton to the distal oxygen via one or two water molecules. In addition, one may have to investigate the rate of water diffusion into the low-density hydration sites near the active site of the protein. Since any of these steps may be rate determining, the contribution of the Asp-251 conformational fluctuation to the overall rate of proton delivery cannot be assessed easily. The present method identifies an extensive set of *possible* proton conduction pathways for proteins of known structure and provides crude estimates of their energetic and kinetic feasibility. Those pathways then need to be verified experimentally, or in detailed calculations, by determining the contributions of individual steps to the overall rate of proton delivery.

Acknowledgment. G.H. wants to thank Prof. Mårten Wiktsröm and Prof. Regis Pomès for many discussions on biomolecular proton transfer. A preliminary account of this work was presented at the "Statphys-Kolkata IV Meeting", Kolkata, India, January 14-19, 2002 (appeared in the proceedings of the meeting, *Physica A* **2003**, *318*, 293; editors S. S. Manna and J. K. Bhattacharjee).

JA016860C